Int. J. Electrochem. Sci., 17 **(2022)** Article Number: 220210, doi: 10.20964/2022.02.23

International Journal of
ELECTROCHEMICAL
SCIENCE
www.electrochemsci.org

Preparation of MoS_2 and MoO_3 Modified TiO_2 Composites with Enhanced Visible-light Photocatalytic Activity for Dye Degradation

Youfeng Zhang[1,*], *Shasha He*[1], *Zelong He*[1], *Yichen Zhang*[1], *Yaping Feng*[1], *Yinling Wang*[2], *Min Zhang*[3,*]

[1] School of Materials Engineering, Shanghai University of Engineering Science, Shanghai 201620, P. R. China
[2] Henan Engineering Laboratory of New Energy Conversion and Control Technology, Huanghuai University, Zhumadian Henan 463000, P. R. China
[3] School of Chemistry and Chemical Engineering, Shanghai University of Engineering Science, Shanghai 201620, P. R. China
[*]E-mail: Zhangyoufeng@sues.edu.cn; zhangmin@sues.edu.cn

Received: 26 October 2021 / *Accepted:* 3 December 2021 / *Published:* 5 January 2022

TiO_2 is a widely used semiconductor photocatalyst for environmental governance and new energy applications. However, the development of TiO_2 has been hindered by its low utilisation of solar energy and poor quantum efficiency. In this work, a neoteric TiO_2@MoS_2 with a hollow structure and Au coating was designed. The composites showed good synergistic effects and improved visible-light utilisation for of photocatalytic reactions. MoS_2 nanosheets were modified on TiO_2 microtubes to obtain TiO_2@MoS_2 composites with MoS_2 loading amounts of 29wt%, 32wt% and 50 wt%. The TiO_2@MoS_2 (32-wt%) showed a remarkable enhancements in photocatalytic dye degradation compared with TiO_2 microtubes. Au nanoparticles were successfully deposited on TiO_2@MoS_2-32% to achieve TiO_2@MoS_2@Au. The degradation rate of MB by TiO_2@MoS_2@Au was 1.80 and 1.46 times greater than those of TiO_2 and TiO_2@MoS_2-32%, respectively. Morever, the adsorption rate of MB by TiO_2@MoS_2@Au was 7.86 and 1.16 times greater than those of TiO_2 and TiO_2@MoS_2-32%, respectively. This work provides a new process for improving the photocatalytic activity of TiO_2.

Keywords: TiO_2, MoS_2, Au, synergistic effect, visible photocatalysis

1. INTRODUCTION

Rapid growth in industrialisation and the global population, has highlighted the effects of energy shortage and environmental pollution, the exacerbation of which could lead to a global crisis. Thus, the development of non-polluting environmental purification and alternative clean-energy

technologies is an urgent task in efforts to promote the sustainable development of human society. Because of their potential use in energy and environmental applications, semiconductor photocatalysts are often included in projects related to "Green Earth" and renewable energy; indeed, these materials have been widely studied by a great many scholars. TiO_2 is the most widely studied semiconductor photocatalyst; it has been applied as a semiconductor material in environmental governance and new energy because of it is inexpensive, non-toxic and corrosion resistant [1-8]. However, TiO_2 is not a perfect photocatalyst. First, because of its wide bandgap (~ 3.2 eV), it can only absorb ultraviolet (UV) light, which accounts for only 5% of the full spectrum of sunlight. Thus, TiO_2 is unable to utilize solar energy fully. Second, the electrons and holes generated by the light excitation of TiO_2 can easily recombine, resulting in low quantum efficiency. Several methods, such as element doping [9], dye sensitisation [10-12], semiconductor complexation [13,14], and surface precious metal deposition [15,16], amongst others, have been developed to extend the photoresponse range of TiO_2 to the visible region and improve its photocatalytic quantum efficiency.

MoS_2 is a type of co-catalyst with excellent performance, which is attributed to its typical layered structure. It has broad application prospects in the fields of photochemistry and photocatalysis. TiO_2 sensitised with MoS_2 nanoclusters has been found to show superior visible-light catalytic performance [17-19]. Zhou et al. synthesised TiO_2 nanobelt composites coated with MoS_2 (2H) nanosheets via a two-step hydrothermal method at 200 °C using sodium molybdenum and thioacetamide; the resultant materials exhibited strong photocatalytic activity and visible-light absorption on account of their high carrier separation efficiency [20]. Bulk Au cannot easily be reacted with other molecules because of its high ionisation potential. However, Au shows excellent catalytic activity in the nanometer scale [21, 22]. The deposition of Au nanoparticles on TiO_2 can change the electron distribution of the latter and modulate its surface properties to achieve the effective separation of photogenerated electrons and holes. Such separation making the electrons migrating to the surface of Au reduction reaction, such as hydrogen production, and the holes remaining in the valence oxidation reaction, such as the degradation of dyes. Murdoch et al. deposited Au nanoparticles of different sizes on TiO_2 using a precipitation deposition method, and systematically studied the effects of Au nanoparticles on the photocatalytic hydrogen production of Au/TiO_2 [23].

The step-wise modification of TiO_2 is a research hot spot in the field of semiconductor photocatalysis. In this work, neoteric $TiO_2@MoS_2$ with a hollow structure and Au coating was designed to improve the photocatalytic activity of TiO_2. The advantages of this design are described below. Firstly, MoS_2 nanosheets were modified on TiO_2 microtubes by a one-step hydrothermal method to obtain $TiO_2@MoS_2$ [14]. Photocatalytic reactions can occur on the outer and inner surfaces of the composite because of its hollow structure, and the efficiency of light capture is promoted by light radiation from the internal cavity. Secondly, Au nanoparticles were introduced to the composites to synthesise $TiO_2@MoS_2@Au$. Incorporation of Au nanoparticles into $TiO_2@MoS_2$ microtubes could provide materials with excellent stability, which originates from the improved adsorbability of visible light. Each component of the multifunctional $TiO_2@MoS_2@Au$ nanocomposite demonstrated complementary properties, resulting in improvements in the light utilisation rate of TiO_2.

2. EXPERIMENTAL DETAILS

2.1. Materials

Ammonium molybdate (VI) tetrahydrate ($(NH_4)_6MoO_{24}\cdot 4H_2O$, 99%), nitric acid ($HNO_3$, 65%), titanium oxysulfate ($TiOSO_4$), 93%), thiourea (NH_2CSNH_2, 99%), molybdenum trioxide (MoO_3, 99.99%) and hydrogen tetrachloroaurate(III) trihydrate ($H_7AuCl_4O_3$, 99.99%) were purchased from Shanghai Titan Technology Co., Ltd, China. All other materials used in this work were of analytical grade.

2.2. Synthesis of MoO_3 microrods

Exactly 1 g of $(NH_4)_6Mo_7O_{24}\cdot 4H_2O$) was dispersed in 20 mL of deionised water under 5 minutes. Next, 5 mL of concentrated HNO_3 (65%) was poured into the prepared solution. The above mixed solution was poured into a 50 mL Teflon hydrothermal reactor, placed in an auto-programmed oven at 180 ℃ keeping 20 h, and then cooled naturally to room temperature. Finally, the product was collected by centrifugation for 5 min, washed with a mixture of ethanol and water and dried at 60℃ for 12 h.

2.3. Preparation of MoO_3@TiO_2 microcables and TiO_2 microtubes

The titanium source is 25 mL of 0.2 mol/L titanium $TiOSO_4$ in ethanol solution. 0.15 g of the as-prepared MoO_3 microrods was dispersed in 100 mL of deionised water. Next, then titanium source was dropped into the MoO_3 solution with Vigorous stirring for 5 h. After standing for 3 h, the products were separated by centrifugation and washed thrice with a mixture of ethanol and water. Finally, the composite was obtained by drying at 60℃ for 12 h.

The as-prepared MoO_3@TiO_2 microcables (50 mg) were dispersed in 25 mL of anhydrous ethanol solution and 15 mL of deionised water. Next, 1.5 mL ammonium hydroxide was dropped into the above solution, and the mixture was stired for 7 min. Finally, the TiO_2 microtubes were obtained by centrifugation and drying.

2.4. Preparation of TiO_2@MoS_2 composites and MoS_2 nanosheets

Exactly 0.3425 g of NH_2CSNH_2 was dispersed in 30 mL of deionised water as solution A. Next, 30 mg of the as-prepared MoO_3@TiO_2 microcables and 18.75 mg of MoO_3 powders were added to the solution A under ultrasonication for 5 min. Do not add the as-prepared MoO_3@TiO_2 when synthesizing MoS2 nanotablets. The above mixture solution was poured into a 50 mL Teflon hydrothermal reactor and placed in an auto-programmed oven at 200°C for 24h. The mixture was cooled naturally to room temperature, centrifuged for 5 min to obtain the composites and washed thrice with a mixture of ethanol and water. The resultant TiO_2@MoS_2 composite (32 wt% MoS_2) was obtained by drying at 60°C for 12h. The masses of MoO_3 (were varied to 37 and 0 mg) to obtain

TiO_2@MoS_2 composites with MoS_2 loading amounts of 50 wt% and 29 wt%, respectively.

2.5. Preparation of TiO_2@MoS_2@Au composite

Exactly 10 mg of as-prepared TiO_2@MoS_2-32% was dispersed into 20 mL of deionised water under sonication as solution A. Next, 4 mg of $HAuCl_4 \cdot 3H_2O$ was dispersed into 10 mL of deionised water under sonication as solution B. Solution B was added drop-wise into solution A, and ultrasound treatment was continued for 1 h. Finally, TiO_2@MoS_2@Au was obtained by centrifugation and drying.

2.6. Characterization

The X-ray diffraction (XRD) with Co Kα radiation (X'Pert PRO, PANalytical, Holland) was used to measure crystal structures. The element types of materials were determined by X-ray photoelectron spectroscopy (XPS), the model is a Kratos analytical instrument (ESCALAB 250Xi). Scanning electron microscopy (SEM) (S-3400, Hitachi, Japan) was used to characterize surface microstructure of as-synthetic products. The UV-Visible spectrum of reflectance spectrum of the adsorbed solution was determined by UV-Visible spectrophotometer (Evolution 201). The UV-Vis diffuse reflectance spectra (DRS) of the samples were measured by a UV-Vis diffuse reflectance apparatus (UV-3600) made by Shimazu Company in Japan, with the range of 200~800nm and with $BaSO_4$ as the reflectance standard.

2.7. Photocatalytic activity test

The photocatalytic performance of the prepared samples was evaluated by degrading methylene blue solution (MB) in a photoreactor system under 300W xenon lamp. 5 mg photocatalyst was placed in a quartz reactor with 40 mL, 10 mg/L MB aqueous solution, and then magnetically stirred in the dark for 2 h to achieve the adsorption-desorption equilibrium. Once illumination started, samples were sampled every 20 min and the absorption spectrum of the MB solution was measured using an UV-Vis spectrophotometer (Evolution 201) with a wavelength range of 400-800nm.

3. RESULTS AND DISCUSSION

Fig. 1 shows the XRD patterns of MoO_3, MoO_3@TiO_2, TiO_2@MoS_2 with different MoS_2 loading amounts (50 wt%, 29 wt% and 32 wt%) and TiO_2@MoS_2@Au (32 wt% MoS_2). The curve of MoO_3@TiO_2 is similar to that of MoO_3, which indicates that amorphous TiO_2 is formed during the sol-gel reaction. The curves of TiO_2@MoS_2 present characteristic peaks located at 25.69°, 38.40° and 55.94°, which correspond to the (101), (004) and (211) planes, respectively, of anatase TiO_2 (JCPDS Card No. 75-1537). The peaks located at 14.32°, 33.12°, 49.59°and 58.86° correspond to the (002), (100), (105) and (110) planes, respectively, of anatase MoS_2 (JCPDS Card No. 75-1539). The above

results indicate that the composites are composed of TiO_2 and MoS_2. The characteristic diffraction peak of MoO_3 is not observed in curves of the TiO_2@MoS_2 composites, thereby showing that the MoO_3 as molybdenum source is fully converted into MoS_2. The characteristic peak of Au is also captured in the top spectrum line, thereby indicating that TiO_2@MoS_2@Au was successfully synthesised.

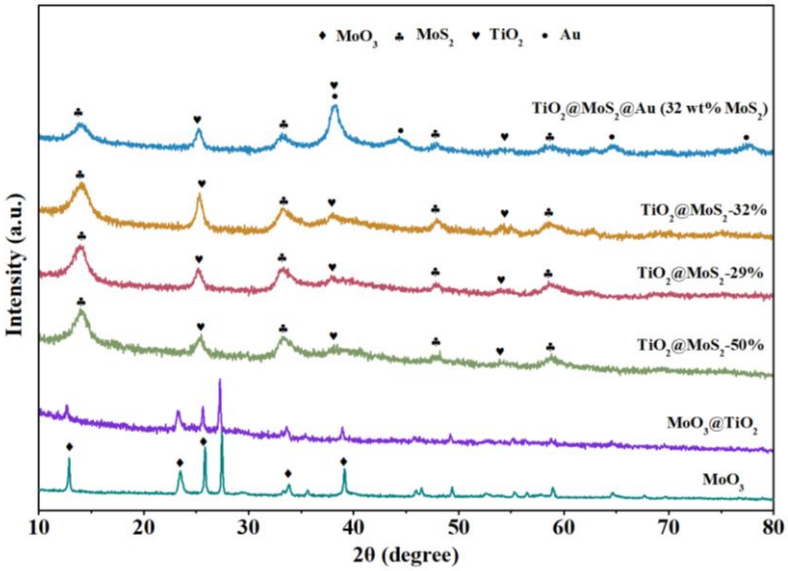

Figure 1. XRD patterns of MoO_3, MoO_3@TiO_2, TiO_2@MoS_2 with different MoS_2 loading amounts (50 wt%, 29 wt% and 32 wt%) and TiO_2@MoS_2@Au (32 wt% MoS_2)

TiO_2@MoS_2@Au (32 wt% MoS_2) was investigated further to confirm its chemical composition and elemental states; the results are shown in Fig. 2. Au, Ti, O, Mo and S were detected in the survey scan of TiO_2@MoS_2@Au (Fig. 2a), Fig. 2 (b) shows the high-resolution XPS spectrum of Ti 2p. The peaks centered at 459.87 and 475.55 eV are attributed to the Ti^{4+} $2p_{3/2}$ and $2p_{1/2}$ states of TiO_2@MoS_2@Au. Fig. 2 (c) shows the high-resolution XPS spectrum of O 1s. The O 1s peak of TiO_2@MoS_2@Au is located at 531.12 eV and could be attributed to Ti-O bonding. The peak located at 532.57 eV reflects the presence of oxygen vacancies and adsorbed water molecules [24-27]. The Fig. 2(b) and 2 (c), confirm the presence of TiO_2 in the composite. Fig. 2(d) shows the high-resolution XPS spectrum of Mo 3d. The peaks centered at 229.70 and 232.87 eV are Mo $3d_{5/2}$ and Mo $3d_{3/2}$ states of element Mo respectively, thus confirming the presence of Mo^{6+} in MoS_2. A shoulder peak appears at 226.91 eV, which corresponds to S2s [26]. The high-resolution XPS spectrum of S is shown in Fig. 2(e). Here, the MoS_2 layers of TiO_2@MoS_2@Au contain atoms S with electron binding energies of 162.55(S $2p_{3/2}$) and 163.70 eV (S $2p_{1/2}$). The results in Figs. 2(d) and 2 (e), reflect the presence of MoS_2 in the composite. The high-resolution XPS spectrum of Au 4f is given in Fig. 2(f). Here, the peaks centered at 84.75 and 88.40 eV are attributed to the Au $4f_{7/2}$ and $4f_{5/2}$ states, respectively, of TiO_2@MoS_2@Au. The above XPS results confirm that TiO_2@MoS_2@Au was successfully formed consistent with the XRD results.

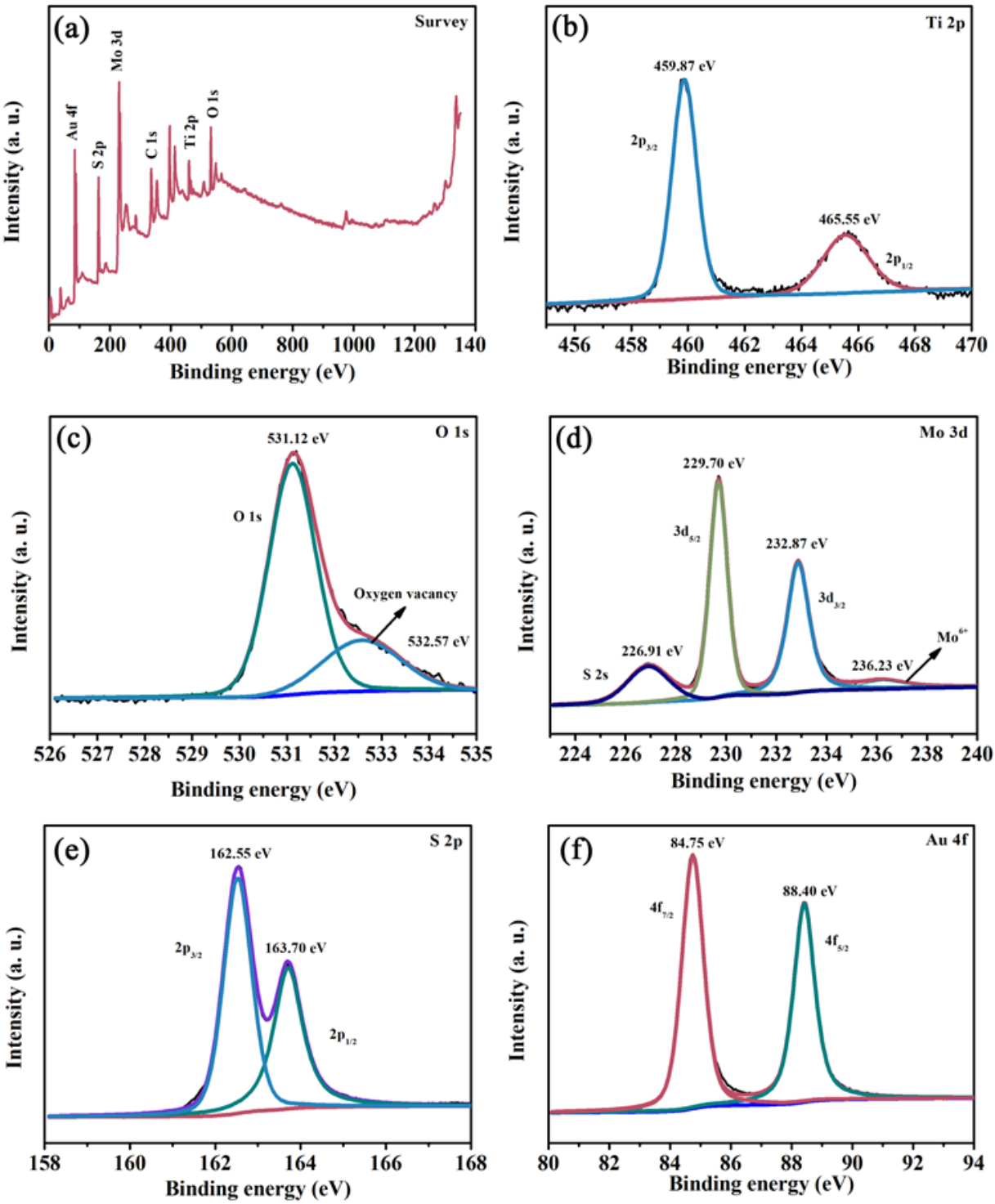

Figure 2. XPS spectra of (a) fully scanned spectra, (b) Ti 2p, (c) O 1 s, (d) Mo 3d, (e) S 2p and (f) Au 4f in @TiO_2@MoS_2@Au composites (32 wt% MoS_2)

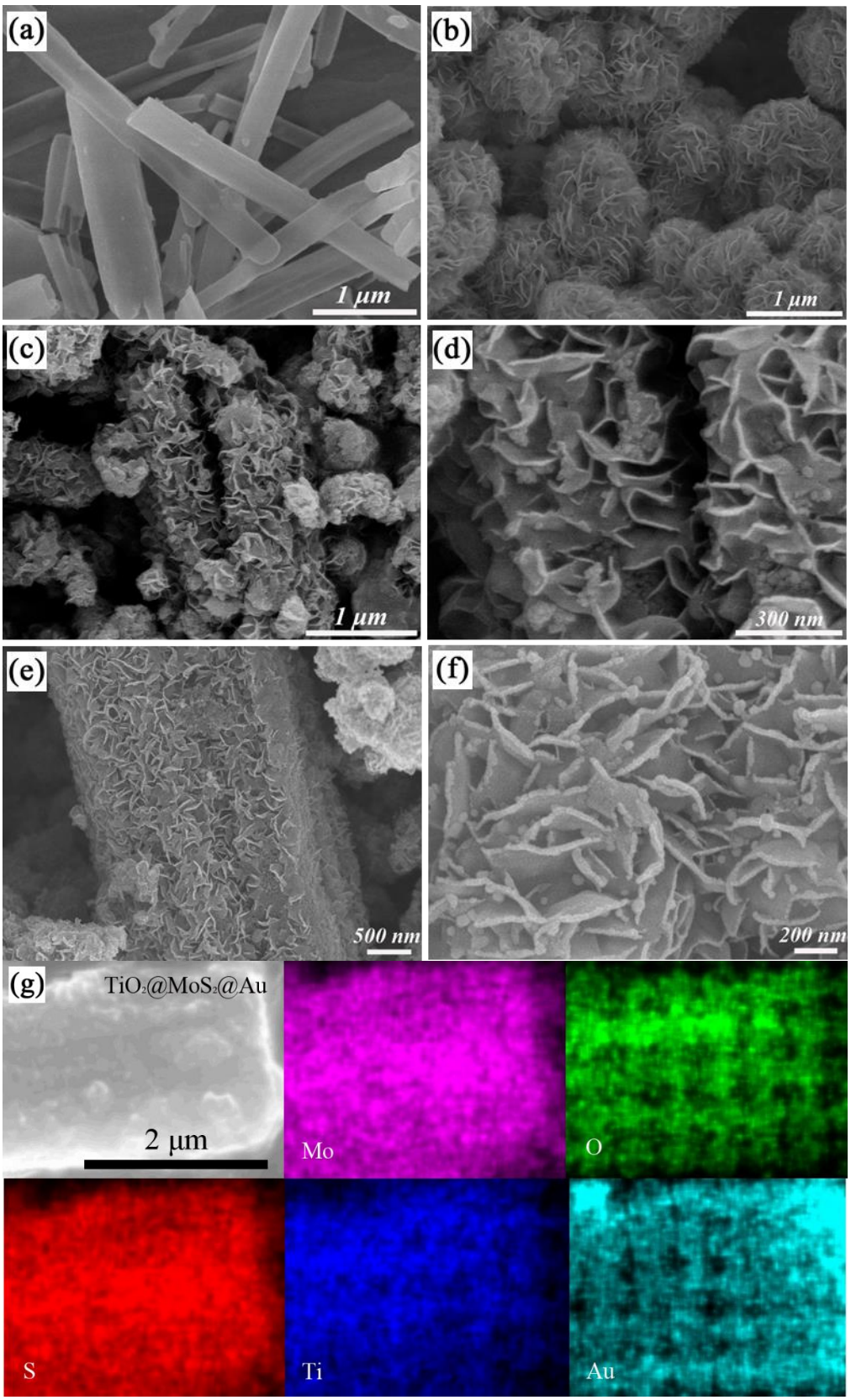

Figure 3. Scanning electron microscopy images of (a) TiO_2, (b) MoS_2, (c, d) TiO_2@MoS_2 (32 wt% MoS_2), and (e, f) TiO_2@MoS_2@Au (32 wt% MoS_2. (g) EDS elemental maps of TiO_2@MoS_2@Au.

The morphologies of TiO_2, MoS_2, TiO_2@MoS_2 composites with different MoS_2 loading amounts and TiO_2@MoS_2@Au (32 wt% MoS_2) were characterised by SEM (Figs. 3 and S1). As shown in Figs. 3(a) and 3(b), individual TiO_2 presents a 1D microtube shape whilst individual MoS_2 presents a nanosphere-like shape assembled with nanosheets. The TiO_2@MoS_2 composites were formed through sulfidation. As shown in Figs. S1 (a) and S1(c), the MoS_2 nanosheets in TiO_2@MoS_2-50% are quite abundant whereas the MoS_2 nanosheets in TiO_2@MoS_2-29% are relatively limited. As shown in Figs. 3(c) and 3(d), a moderate quantity of MoS_2 is uniformly distributed on the TiO_2 microtube. Au was deposited on TiO_2@MoS_2-32% for further modification. As shown in Figs. 3(e) and 3(f), the Au nanoparticles are well dispersed on the MoS_2 nanosheets. The EDS elemental distributions shown in Fig.3(g) reflect the uniform distribution of Mo, O, S, Ti and Au elements on TiO_2@MoS_2@Au.

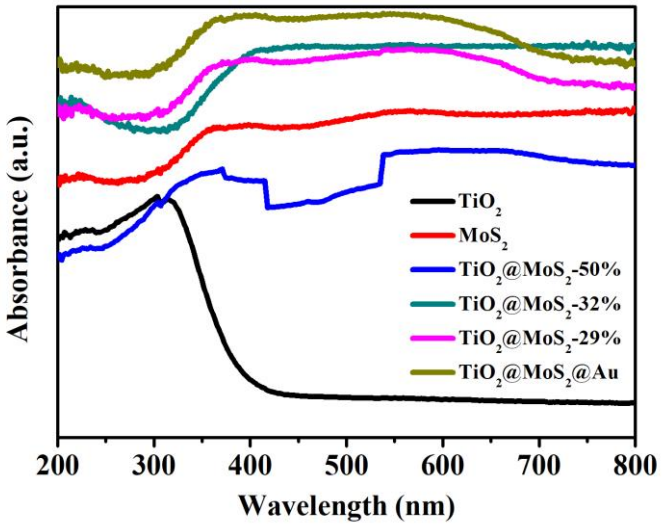

Figure 4. UV-vis absorption spectra of TiO_2, MoS_2, TiO_2@MoS_2 composites with different MoS_2 loading amounts and TiO_2@MoS_2@Au (32 wt% MoS_2)

The photocatalytic property of a material largely depends on its light absorption performance. The Fig.4 gives UV-vis absorption spectra of materials using solar lamp capturing. The visible-light absorption range of MoS_2 increased because of it is black feature [28]. Due to TiO_2 is antase structure, it has a good absorption in the UV range, but bad in the visible-light range [29]. The optical absorption of coupled TiO_2@MoS_2 with different MoS_2 loading amounts is distinctly increased in the both of UV and visible-light ranges, thereby possibility of capture photons was obviously facilitated because of the heterostructure. Amongst the optical absorption values of the TiO_2@MoS_2 composites, the TiO_2@MoS_2-32 is highest. After coating with Au, the optical absorption of TiO_2@MoS_2@Au is significantly enhanced compared with those of the TiO_2@MoS_2 composites. The absorption can not only be put down to dual absorption of MoS_2 in the UV and visible-light ranges, but also be reflected back by the dark feature of the TiO_2@MoS_2@Au [26]. Using semiconductor band gap formula ($(\alpha h\nu)^n$) and the energy of exciting light ($h\nu$) can be acquired the band gap energy (Eg) of TiO_2. The

estimated Eg of TiO_2, TiO_2@MoS_2-32% and TiO_2@MoS_2@Au are 3.26, 3.05 and 1.57 eV (Fig. S2), respectively.

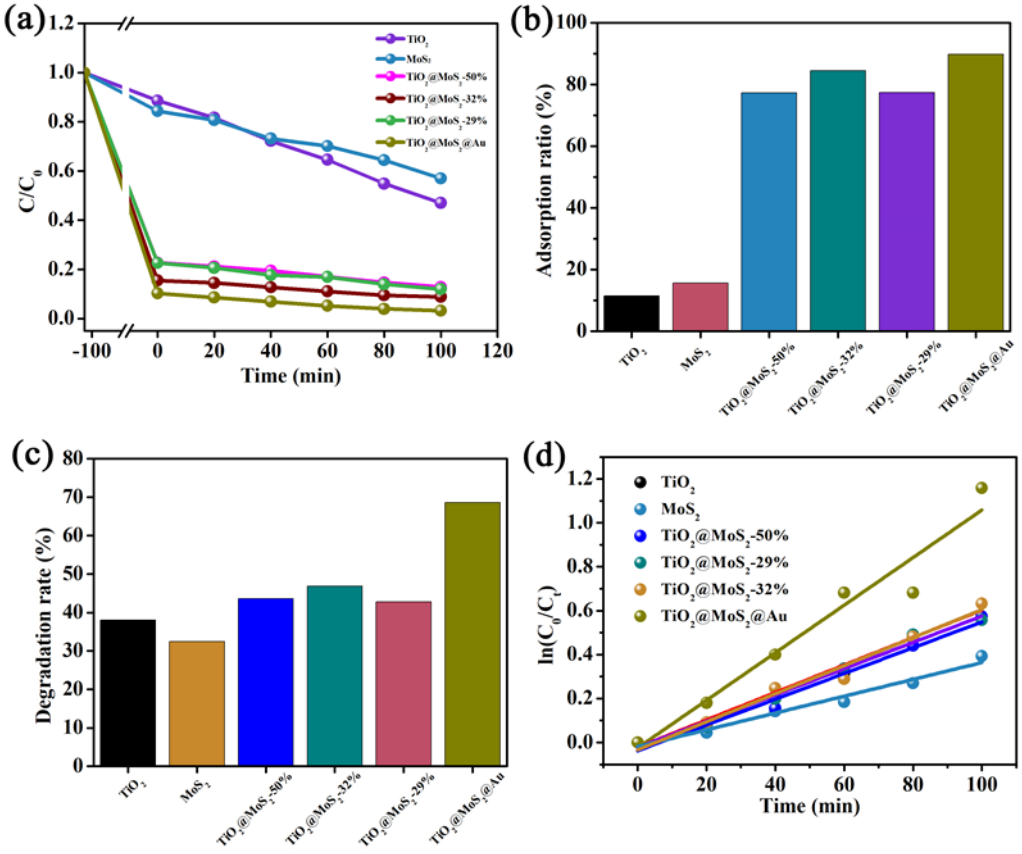

Figure 5. (a) Removal efficiency, (b) MB adsorption rate in the dark after stirring, (c, d) photocatalytic degradation of MB under visible light irradiation with TiO_2, MoS_2, TiO_2@MoS_2 composites (50 wt%, 29 wt% and 32 wt% MoS_2) and TiO_2@MoS_2@Au composite

The photocatalytic activity of the different composites towards dye degradation was evaluated under the simulated light provided by a 300 W Xe arc lamp. Fig. 5 compares the photocatalytic dye degradation activities of TiO_2, MoS_2, TiO_2@MoS_2 (29 wt%, 32 wt% and 50 wt% MoS_2) and TiO_2@MoS_2@Au. As shown in Fig. 5(a), the dye adsorption rates of the TiO_2@MoS_2 composites are higher than that of monomer TiO_2; amongst the adsorption rates of the TiO_2@MoS_2 composites that of TiO_2@MoS_2-32% is the highest. When Au is combined with TiO_2@MoS_2-32%, the removal efficiency is enhanced to 96.78%. The composites have higher adsorption capacity than TiO_2 because of the large specific surface area and adsorption capacity of MoS_2 [30]. As shown in Fig. 5(b), the adsorption ratio of TiO_2@MoS_2-32% reaches 84.49%, whilst that of TiO_2@MoS_2@Au reaches 89.73%. Fig. 5(c) shows the photocatalytic degradation rate of MB under visible light. The degradation ratio of TiO_2@MoS_2-32% reaches 46.85%, whilst that of TiO_2@MoS_2@Au reaches 68.60% after 100 min of irradiation. Fig. 5(d) illustrates the relationship between $\ln(C_0/C_t)$ and illumination time; here, C_t is the concentration of MB at time t and C_0 is the initial photocatalytic concentration of MB. The

figure reveals that the photocatalytic reaction process conforms to a first-order kinetic process, and that photocatalytic reaction rates of TiO_2@MoS_2@Au is as high as 0.01083 min^{-1}, which is 1.70 times higher than that of the TiO_2 monomer. These results show that co-modification with MoS_2 and Au can enhance the photocatalytic activity and efficiency of TiO_2. The comparison of the degradation capacities for MB on various adsorbents is given in Table 1. The good degradation ratio is represented in MoS_2 and MoO_3 modified TiO_2 Composites.

Table 1. The comparison of the degradation capacities for MB on various adsorbents

catalysts	Degradation Ratio (%)	Ref.
MoS_2/graphene/N-TiO_2 composites (MGNT)	11.10	[2]
CuO/TiO_2	58.4	[5]
$ZnTiO_3$/TiO_2	56.60	[7]
$Ag_6Si_2O_7$/TiO_2	98.60	[8]
TiO_2@MoS_2@Au	68.60	This work

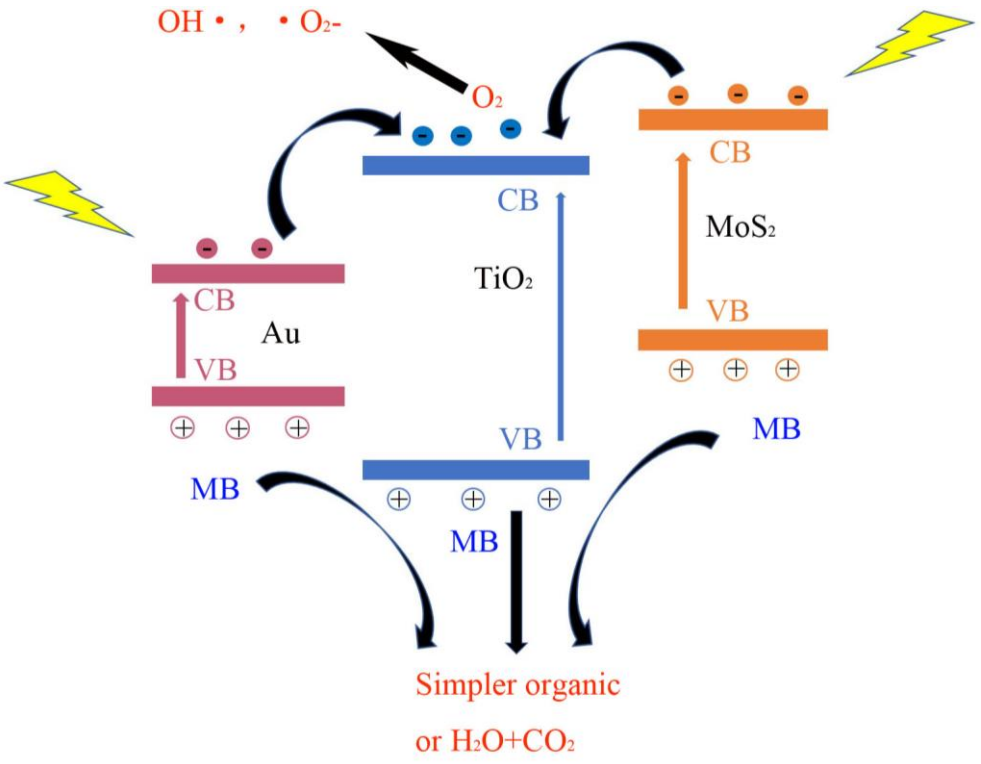

Figure 6. Proposed mechanism for the photocatalytic degradation of MB by TiO_2@MoS_2@Au composites.

Fig.6 shows a probable mechanism for the photocatalytic degradation of MB by TiO_2 composites modified with MoS_2 and Au. The synergistic effects of MoS_2 and Au on TiO_2 on the improvement in the photocatalytic activity of TiO_2 may be attributed to three aspects. (1) The MoS_2 nanosheets can sensitise TiO_2, and endow it with excellent photocatalytic performance under visible light [31]. (2) Au nanoparticles have a separate absorption peak in the visible region. When Au is deposited on the TiO_2@MoS_2 composites, TiO_2@MoS_2@Au can make full use of the visible light spectrum to enhance the catalytic activity of the composite [32-34]. (3) A Schottky junction is formed between Au nanoparticles and TiO_2 interface, thereby hindering the reformation of photogenerated electron hole pairs and improving the photocatalytic effect of the composite[16].

5. CONCLUSIONS

TiO_2@MoS_2 photocatalysts were synthesised via a one-step hydrothermal method, and Au nanoparticles were successfully deposited on TiO_2@MoS_2-32% to obtain TiO_2@MoS_2@Au as a photocatalyst. Co-modification with MoS_2 and Au improved the photocatalytic activity of TiO_2 under visible light. Compared with TiO_2 and TiO_2@MoS_2, the TiO_2@MoS_2@Au could be activated by light irradiation to generate more electron hole pairs improve the photocatalytic activity of TiO_2. Under visible light irradiation for 100 min, the degradation rate of MB by TiO_2@MoS_2@Au was 68.60%, which is 1.80 and 1.46 times greater than those of TiO_2 and TiO_2@MoS_2-32%, respectively. Moreover, the adsorption rate of MB by TiO_2@MoS_2@Au was 89.73%, which is 7.86 and 1.16 times greater than those of TiO_2 and the TiO_2@MoS_2-32%, respectively. This study provides a new process for improving the photocatalytic activity of TiO_2 and presents an alternative method for preparing novel photocatalysts.

ACKNOWLEDGEMENTS
This work was supported by the Nature Science Foundation of China (No.11604204).

SUPPORTING MATERIAL

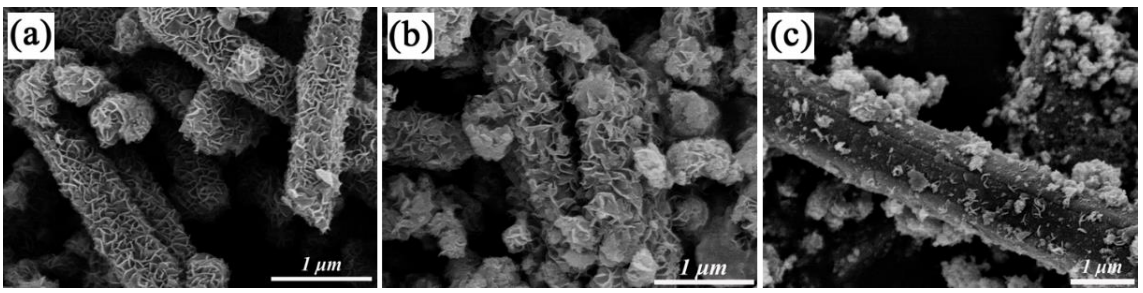

Figure S1. SEM images of TiO_2@MoS_2 composites with different MoS_2 loading amount (a) 50 wt%, (b) 32 wt% and (c) 29 wt%.

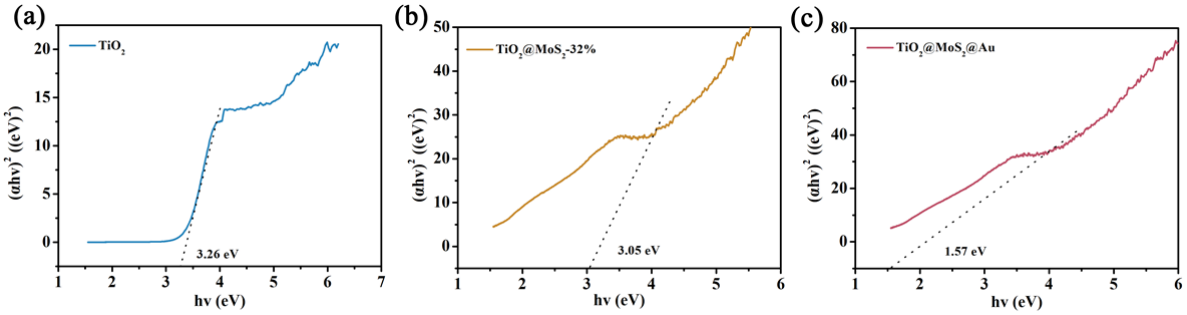

Figure S2. Band gap values of (a) TiO_2, (b) TiO_2@MoS_2 composites (32 wt% MoS_2) and TiO_2@MoS_2@Au composites (32 wt% MoS_2).

References

1. G. Liu, H. G. Yang, J. Pan, Y. Q. Yang, G. Q. Lu and H. M. Cheng, *Chem Rev*., 114 (2014) 9559.
2. X. Lin, M. Sun, M. Hu, Y. Yao, W. Wang, *Mater. Reports*, 32 (2018) 1213-1217+1235.
3. W. J. Ong, L. L. Tan, S. P. Chai, S. T. Yong and A. R. Mohamed, *Nanoscale*, 6 (2014) 1946.
4. Y. Lan, Y. Lu and Z. Ren, *Nano Energy*, 2 (2013) 1031.
5. X.M. Wu, J.J. Yu, J. Xuchang. *J. Sichuan. Univ* ., 34(2015) 87-92.
6. H. Xu, S. Ouyang, L. Liu, P. Reunchan, N. Umezawa and J. Ye, *J Mater Chem* A., 2 (2014) 12642.
7. L. Liu, Y.E. Du, J. Li, Y.F. Liu, X.M. Cai, Y.Q. Chne, *J. Sichuan. Univ.,* 55 (2018) 827-832.
8. W. Jiang, H. Mo, T. Fan, Z. Zhao, Y. Ren, C. Wang, W. Zhang, C. Zang, *J. Text. Res.,* 42 (2021) 107-113.
9. Z. Hong, M. Wei, T. Lan, L. Jiang and G. Cao, *Energy Environ Sci*., 5 (2012) 5408.
10. Z. Bian, T. Tachikawa and T. Majima, *J Phys Chem Lett*., 3 (2012) 1422.
11. A. Ayati, A. Ahmadpour, F. F. Bamoharram, B. Tanhaei, M. Manttari and M. Sillanpaa, *Chemosphere*, 107 (2014) 163.
12. P. Christopher, H. Xin, A. Marimuthu and S. Linic, *Nat Mater*., 11 (2012) 1044.
13. S. Linic, P. Christopher and D. B. Ingram, *Nat Mater*., 10 (2011) 911.
14. S. He, Y. Zhang, J. Ren, B. Wang, Z. Zhang and M. Zhang, *Colloid Surface* A., 600 (2020) 124900.
15. L. Liu, S. Ouyang and J. Ye, *Angew Chem Int., Edit*., 52 (2013) 6689.
16. D. Ding, K. Liu, S. He, C. Gao and Y. Yin, *Nano Lett*., 14 (2014) 6731.
17. W. Ho, J. C. Yu, J. Lin, J. Yu and P. Li, *Langmuir*, 20 (2014) 5865.
18. M. Zhang, Y. Ling, L. Liu, J. Xu, J. Li and Q. Fang, *Inorg Chem Front*., 7 (2020) 3081.
19. J. Zheng, D. Song, H. Chen, J. Xu, N. S. Alharbi, T. Hayat and M. Zhang, *Chinese Chem Lett*., 31 (2020) 1109.
20. W. Zhou, Z. Yin, Y. Du, X. Huang, Z. Zeng, Z. Fan, H. Liu, J. Wang and H. Zhang, *Small*, 9 (2013) 140.
21. M. Haruta, *Cattech.*, 6 (2002) 102.
22. D. T. Thompson, *Nano Today*, 2 (2007) 40.
23. M. Murdoch, G. I. Waterhouse, M. A. Nadeem, J. B. Metson, M. A. Keane, R. F. Howe, J. Llorca and H. Idriss, *Nat Chem*., 3 (2011) 489.
24. K. K. Paul, N. Sreekanth, R. K. Biroju, A. J. Pattison, D. Escalera-López, A. Guha, T. N. Narayanan, N. V. Rees, W. Theis and P. K. Giri, *J Mater Chem* A., 6 (2018) 22681.
25. S. S. M. Bhat, S. A. Pawar, D. Potphode, C.-K. Moon, J. M. Suh, C. Kim, S. Choi, D. S. Patil, J.-J. Kim, J. C. Shin and H. W. Jang, *Appl Catal B-Environ*., 259 (2019) 118102.
26. Y. Li, Z. Yin, G. Ji, Z. Liang, Y. Xue, Y. Guo, J. Tian, X. Wang and H. Cui, *Appl Catal B-Environ*., 246 (2019) 12.

27. M. Zhang, L. Ding, J. Zheng, L. Liu, H. Alsulami, M. A. Kutbi and J. Xu, *Appl Surf Sci*., 509 (2020) 145348.
28. L. Yuwen, F. Xu, B. Xue, Z. Luo, Q. Zhang, B. Bao, S. Su, L. Weng, W. Huang and L. Wang, *Nanoscale*, 6 (2014) 5762.
29. Z. Liang, X. Bai, P. Hao, Y. Guo, Y. Xue, J. Tian and H. Cui, *Appl Catal B-Environ*., 243 (2019) 711.
30. X. Hu, S. Lu, J. Tian, N. Wei, X. Song, X. Wang and H. Cui, *Appl Catal B-Environ*., 241 (2019) 329.
31. C. Peng, P. Wei, X. Li, Y. Liu, Y. Cao, H. Wang, H. Yu, F. Peng, L. Zhang, B. Zhang and K. Lv, *Nano Energy*, 53 (2018) 97.
32. P. Christopher, H. Xin, A. Marimuthu and S. Linic, *Nat Mater*., 11 (2012) 1044.
33. S. Linic, P. Christopher and D. B. Ingram, *Nat Mater*., 10 (2011) 911.
34. L. Liu, S. Ouyang and J. Ye, *Angew Chem*., 125 (2013) 6821.